Spectral Disentangling Applied to Triple Systems: RV Crt ⋆

H. Hensberge[1], L.P.R. Vaz[2], K.B.V. Torres[2] and T. Armond[2]

[1] Royal Observatory of Belgium, Ringlaan 3, B-1180 Brussels, Belgium
herman.hensberge@oma.be
[2] Universidade Federal de Minas Gerais, DF-ICEx, C.P. 702,
30.123-970 Belo Horizonte, MG, Brazil lpv@fisica.ufmg.br

Summary. The eclipsing triple system RV Crt shows a composite spectrum dominated by the sharp-lined late-F type spectrum of the tertiary. The spectral lines of the close binary are considerably broadened, since both components rotate synchronously with the orbit. The Doppler shifts and the component spectra are successfully recovered by application of the spectral disentangling technique. The cooler, less massive component of the close binary is larger than the hotter one. The hotter component of the close binary is very similar to the tertiary. The system is probably still on its way to the zero-age main sequence.

1 Introduction

Spectral disentangling is a powerful analysis method for composite spectra, solving self-consistently for N time-independent component spectra and their time-dependent (orbital) Doppler shifts $\Delta\lambda(t_j)$. The relative contribution ℓ_n of each component may depend on time:

$$S_{obs}(t_j) = \sum_{n=1}^{N_{comp}} \ell_n(t_j) S_n\left(\lambda; \Delta\lambda(t_j)\right) \quad (1)$$

The numerical solution was first formulated in velocity space (logarithm of wavelength) by [6] and soon thereafter by [3] using the Fourier components of the spectra. These methods solve for the contribution of each component to the composite spectra. In the case of time-dependent relative contributions $\ell_n(t_j)$, the normalized intrinsic component spectra are reconstructed straightforwardly. Without relative light variability, a unique normalization depends on external information. The most favourable case in the latter situation occurs when all components have at least one very deep absorption line (e.g. Ca II K in cool stars, see [2], [1]), since the requirement that absorption lines should have non-negative flux in any of the components is then sufficient to derive accurate ℓ_n. Recent reviews on applications to observed and artificial data are published in [4]. Note that several numerical codes are available to interested users: the Fourier analysis code KOREL maintained by Hadrava (www.asu.cas.cz/∼had/korel.html), that also deals with hierarchical orbits; and a Fourier analysis code for two (fdbinary) and three components (fd3, preliminary

⋆Based on observations obtained at the European Southern Observatory (ESO), La Silla, Chile

version, `sail.zpf.fer.hr/fdbinary/fd3`) and a spectral separation code (known orbit) in velocity space (`sail.zpf.fer.hr/cres`) maintained by Ilijić.

2 Data

Forty-one high-resolution spectra obtained with the FEROS spectrograph at the 2.2 m ESO telescope, covering adequately the wavelength interval 390–880 nm with a pixel size of $2.7\,\mathrm{km\,s^{-1}}$, are analysed. The 20 min exposures, one of which is obtained during the 25 min totality in the primary eclipse, have a signal-to-noise ratio above 100 (Fig. 1). They cover well all orbital phases at which the line profiles (averaged over the visible stellar disks) are not affected by partial eclipses.

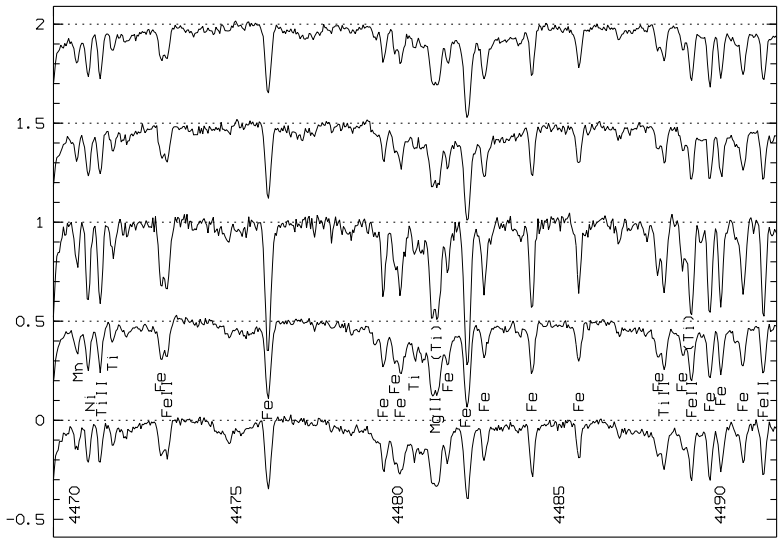

Fig. 1. Detail of the observed spectrum of RV Crt at orbital phases 0.75, 0.875, 0.00, 0.125 and 0.25 respectively (top to bottom). Vertical shifts in relative intensity are applied for clarity. The sharp-lined third component dominates the composite spectrum. Note its stronger, less diluted lines in primary mid-eclipse. The primary is easiest seen near Fe I $\lambda\,4476$, red-shifted in the upper spectra and blue-shifted in the lower ones, and in the moving, broad underlying absorption around $\lambda\,4481$

The orbital period of 1.17050239 d ($\pm 2.1\,10^{-7}$ d) is accurately known from Strömgren *uvby* photometry obtained with the Danish SAT telescope at ESO in 61 nights from 1987 to 1989.

We use the KOREL code. The Fourier analysis technique requires the selection of wavelength regions with edges in (quasi)-continuum. Each region should also con-

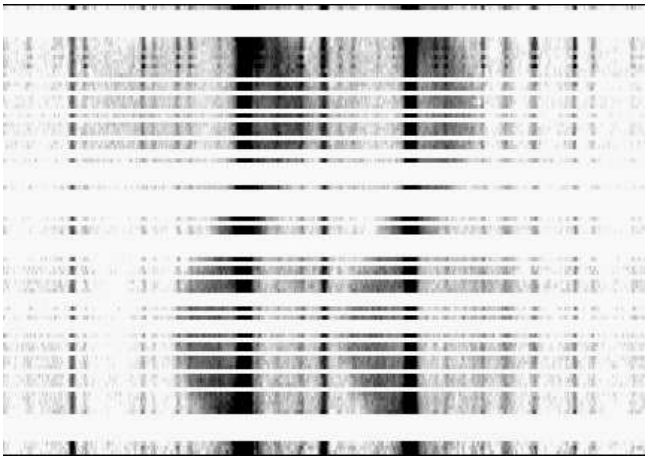

Fig. 2. Visibility of the close binary components in the Na I D lines ($\lambda\lambda\,5890$–5896 Å). Black indicates strong absorption. Orbital phase varies along the vertical axis. Even in these strong lines the contribution of the secondary is only marginally visible (red-shifted in the lower part of the figure, blue-shifted in the upper part)

tain a significantly time-dependent contribution from the close binary component(s) (Fig. 2). We selected 25 regions, with either 512 (3 regions), 1024 (5 regions), 2048 (6 regions) or 4096 (11 regions) spectral bins. Some regions overlap with others. KOREL has been adapted at UFMG to deal at once with all these unequal-length regions. The relative light contributions in each wavelength region were fixed making use of the changes of line strengths in primary mid-eclipse, the light curves, and the light ratios predicted by the associated Wilson-Devinney analysis.

3 Component Spectra

Examples of disentangled component spectra are shown in Fig. 3. The spectrum of the primary mimics the tertiary broadened to the rotation velocity required for synchronization with the orbit. This similarity is a strong indication that the disentangling process is performed properly. The primary and the tertiary contribute equally to the system light near $\lambda\,4000$, and their light ratio depends only slightly on wavelength, e.g. the tertiary is 10% brighter at $\lambda\,5500$. The line widths in the spectrum of the secondary are also in line with synchronization with the orbit. The noise in its intrinsic spectrum is a direct consequence of its faintness, its light contribution (out of eclipse) varying roughly from 4% at $\lambda\,4000$ to 16% of the total system light at $\lambda\,8800$. The different line strengths in the spectrum of the secondary are qualitatively in accordance with its lower stellar temperature ($T_{\rm eff} \approx 4\,200$ K, while primary and tertiary have $T_{\rm eff} \approx 6\,600$ K); but the lack of absorption near 4300 Å might signal a weak G-band of CH (Fig. 3). The possible presence of spectral peculiarities shows how useful is the reconstruction of component spectra without a priori assumptions about spectral features.

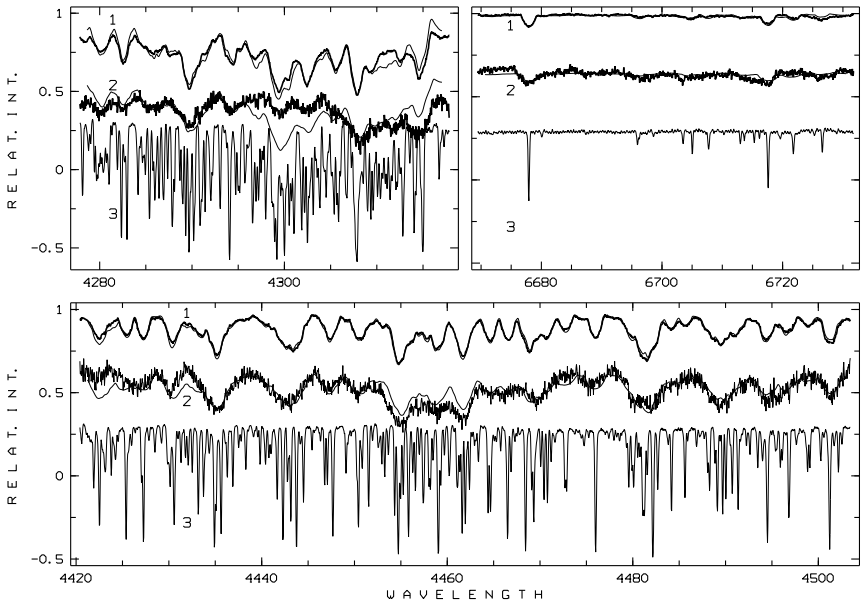

Fig. 3. Disentangled intrinsic component spectra in selected spectral regions. The close-binary component spectra (thick line) are compared to rotationally broadened versions (thin lines) of the tertiary spectrum, assuming rotation synchronous with the orbital period. Note the similarity between primary and tertiary. Shifts in relative intensity are applied to the spectra of the secondary (-0.35) and tertiary component (-0.7)

4 Fundamental Stellar Parameters

Consistent radial velocities are derived from different subsets of regions. In combination with the analysis of the light curves (Figs. 4, 5), they indicate that the secondary (0.41 $M_\odot$, 1.51 $R_\odot$) is less massive, but significantly larger than the primary (0.76 $M_\odot$, 1.13 $R_\odot$). The less massive star is the largest and most overluminous component, confirming that both stars may be contracting to the main sequence [5].

5 Future Work

The present level of disentangling is adequate to derive the orbit and characterize the component spectra. In particular, an accurate mass ratio of the components of the close binary was derived in contrast to earlier attempt using cross-correlation techniques. Nevertheless, minor bias is apparent in the component spectra. An alternative spectral separation, in velocity space, may clarify the role of several effects introducing possibly bias in the component spectra, especially in the fainter one:

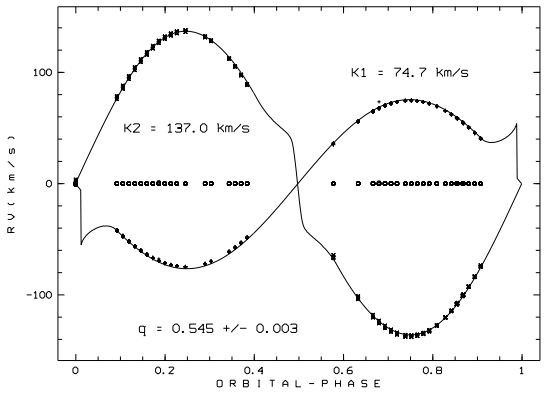

Fig. 4. Radial velocities derived from the subsets of regions with 1024, 2048 and 4096 data points respectively compared to the radial velocity curves computed from the preliminary Wilson-Devinney solution

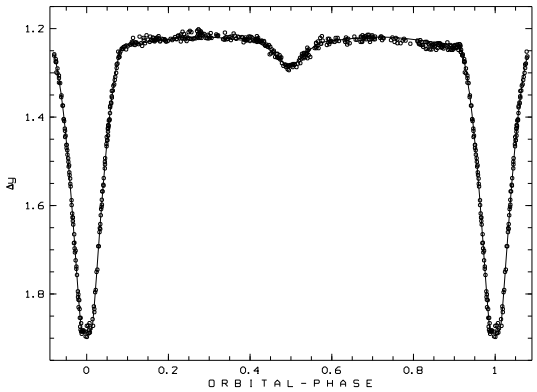

Fig. 5. Differential light-curve in Strömgren y with the Wilson-Devinney solution used in Fig. 4. In both cases low-level systematics in the residuals suggest the need for further refinements

- lack of continuum at the edges of the selected regions;
- masking of telluric lines, interstellar lines (presently only done in the Na I lines) and detector blemishes;
- small bias in the input spectra due to imperfect data reduction.

Indeed, Fourier and velocity space disentangling react different to these issues.

A detailed analysis of the component spectra will provide accurate temperatures and the chemical composition of the atmospheres. Combination of the light curves with spectroscopic temperatures and radial velocities leads to final orbital and stellar parameters, which will be confronted with stellar evolution theory.

Acknowledgments

We are indebted to P. Hadrava for making the KOREL code available. Financial support provided by the Belgian Science Policy (IAP P5/36), and by the Brazilian Agencies CNPq, CAPES and FAPEMIG is acknowledged.

desidera.tex

References

1. Y. Frémat, P. Lampens & H. Hensberge: MNRAS **356**, 545 (2005)
2. R.E. Griffin: AJ **123**, 988 (2002)
3. P. Hadrava: A&AS **114**, 393 (1995)
4. R.W. Hilditch, H. Hensberge & K. Pavlovski (eds.): *Spectroscopically and Spatially Resolving the Components of Close Binary Stars*, ASP Conf. Ser. **318** (2004)
5. A.C. Machado: MSc Dissertation, DF-ICEx-UFMG (1997)
6. K.P. Simon & E. Sturm: A&A **281**, 286 (1994)